Giant, 20, 2024, 100328

Dual role of epoxidized soybean oil (ESO) as plasticizer and chain extender for biodegradable polybutylene succinate (PBS) formulations

Full-length article

Rosa Turco[a,b], Salvatore Mallardo[b], Domenico Zannini[b,c], Arash Moeini[d], Martino Di Serio[a,e], Riccardo Tesser[a,e], Pierfrancesco Cerruti[b,*], Gabriella Santagata[b]

[a] Department of Chemical Sciences, Monte Sant'Angelo Campus, University of Naples "Federico II", Via Cinthia 4, 80126 Naples, Italy
[b] Institute for Polymers, Composites and Biomaterials (IPCB-CNR), National Council of Research, Via Campi Flegrei 34, 80078 Pozzuoli, Italy
[c] Institute of Chemical Sciences and Technologies "Giulio Natta" (SCITEC-CNR), National Council of Research, Via de Marini 6, 16149 Genova, Italy
[d] Research Group of Fluid Dynamics, Chair of Brewing and Beverage Technology, TUM School of Life Sciences, Technical University of Munich, 85354 Freising, Germany
[e] Consorzio Interuniversitario di Reattività Chimica e Catalisi, via Celso Ulpiani 27, 70126 Bari, Italy

Keywords: Polybutylene succinate, Epoxidized soybean oil, Chain extenders, Biodegradable blends, Sustainable packaging

This work reports the effect of 1–5 wt% epoxidized soybean oil (ESO) addition on the thermal, mechanical, and morphological properties of polybutylene succinate (PBS). ESO acts as a chain extender as well as a mild plasticizer of PBS. N-methylimidazole (NMI) is used as a catalyst to promote the reaction between PBS and ESO, and thermal, rheological, and spectroscopic analyses demonstrate increased viscoelastic properties, compatibility, crystallinity and thermal stability of the melt reacted formulations. In the presence of NMI, storage modulus (G') values two orders of magnitude higher than that of pure PBS are achieved, confirming the completion of the chain extension reaction. A drastic refinement of the biphasic structure of the blend is observed, with the formation of a homogenous structure where ESO is well incorporated into the matrix. Finally, tensile tests reveal enhanced mechanical performance in the blends reacted in the presence of NMI. These findings pave the way for the development of a versatile family of materials which could find potential application in sustainable biodegradable packaging.

1 Introduction

Packaging is an essential element of the food industry, capable of protecting and enhancing food products while ensuring the sustainability of the entire production and commercial process related to the sale of food products. Besides acting as physical barrier, packaging shields against contaminants, guaranteeing food integrity and safety, and allowing to extend shelf-life beyond its natural lifespan. Additionally, it provides essential information to consumer for informed choices.

Synthetic polymers, mainly polyesters and polyolefins, including polyethylene terephthalate (PET), low- and high-density polyethylene (LDPE and HDPE) and polypropylene

* Corresponding author.
E-mail address: pierfrancesco.cerruti@cnr.it (P. Cerruti).
Received 30 April 2024; Received in revised form 3 July 2024; Accepted 17 July 2024

 https://doi.org/10.1016/j.giant.2024.100328

(PP), are widely applied for food packaging because of low cost, excellent water resistance, availability and good mechanical and thermo-optical performances [1,2]. However, the still growing tendency to use plastics in the food packaging is responsible for the ever increasing worldwide plastic pollution. The main drawback of conventional polymers is their lack of degradability and compostability. Nowadays, about one-third of plastic waste comprises packaging and short-life materials, and only about 25 % of wasted plastics can be recycled, and the remaining cause environmental and ocean pollution [3]. Therefore, suitable alternatives for non-degradable plastic material, especially in the packaging and cutlery industries, are urgently needed. For this purpose, biopolymers represent a potential alternative to conventional plastics in the food packaging industry because of their biodegradability, renewability, and generally good mechanical properties [4-5]. Biopolymers suitable for food packaging can be either naturally occurring, such as cellulose, starch, alginate, chitosan [6] or produced from renewable sources, as is the case of poly(lactic acid) (PLA), polycaprolactone (PCL), and polybutylene succinate (PBS) aliphatic polyesters [7,8]. Among these biodegradable polymers, PBS is a thermoplastic with properties similar to LDPE (melting temperature about 115 °C, glass transition temperature (T_g) from –40 to –30 °C, heat distortion temperature at 97 °C), making this polymer a promising candidate for food packaging application [9,10]. PBS is synthesized by polycondensation of dimethyl succinate and 1,4-butanediol in different paths; the catalytic reaction is used to obtain higher molecular weight PBS [11,12]. However, obtaining high molecular weight PBS is not an easy task since, just like other aliphatic polyesters, it is subject to a decrease in molecular weight due to hydrolysis and thermal degradation reactions during the post-polymerization processes [13]. These phenomena cause a substantial reduction in the viscosity and melt strength of the polymer, with concomitant decline in mechanical and physical properties [14].

To improve mechanical and thermal performance, PBS requires the use of chain extenders, which are additives able to increase the polymer molecular weight by a post-polymerization reaction during the final step or the mixing, extrusion and injection molding of the final product [15]. Indeed, reactive processing is a frequently used strategy for the cost-effective upgrading of physical and chemical properties of blends of biodegradable polyester such as PLA, PBS, and poly(butylene adipate terephthalate) (PBAT) [16]. In the case of PBS, biscaprolactamate, carbodiimide, and bisoxazoline modifiers, which can couple with the polymer chain ends through their functional groups, are often used as chain extenders [17-19]. To this aim, also fossil-derived epoxy molecules are used as additives able to enhance miscibility and properties of the final product [20,21]. However, in a circular economy approach, epoxidized vegetable oils, such as epoxidized soybean oil (ESO), predominantly made up of triglyceride molecules containing reactive sites like oxirane groups, could be suitably used as chain extenders. Soybean oil is an abundant renewable resource that is cheap and readily available [22], and the use of ESO as a plasticizer has been already established as a valid industrial alternative to the use of low molecular weight phthalates, banned in many countries for their adverse health effects [15,23,24].

In the light of above, in the present study ESO was used as a renewable plasticizer and chain extender to improve PBS thermal stability and mechanical performance by a readily accessible reactive processing extrusion. To this aim, the reactivity of PBS and ESO binary mixtures was first studied using differential scanning calorimetry (DSC). The reaction conditions were then optimized using dodecanedioic acid (DA) as a model compound of PBS, in presence of three different catalysts able to promote the addition of ESO to the PBS chains. Finally, after reaction optimization, the ternary mixtures including PBS, ESO and N-methylimidazole (NMI) as catalyst were extruded, and the obtained reactive blends were thoroughly characterized in their thermal, structural, morphological and mechanical properties, to develop materials with potential applicability in sustainable food packaging.

2 Experimental section

2.1 Materials and chemicals

Polybutylene succinate (poly(1,4-butylene succinate), PBS), M_n ~ 65000 g/mol, and M_w ~100000 g/mol, was supplied by Novamont (Novara, Italy). The polymer was carboxy-terminated, with a content of COOH terminal group of 77 meq/kg. ESO, with a Oxirane Number of 6.1 $mol_{epoxide}$/100 $g_{product}$, was obtained by epoxidation of soybean oil in a fed-batch reactor, using performic acid formed in situ, according to the experimental procedure described in [25]. N-methylimidazole (NMI), dodecanedioic acid (DA), and titanium tetraisopropoxide ($Ti(OPr)_4$) were supplied by Sigma-Aldrich, Methyl trioctylammonium chloride (MTOAC) was provided by Honeywell Fluka.

2.2 Study of the addition reaction of ESO on PBS chains: catalyst screening and preparation of DA/ESO catalyzed mixtures

The reactivity of PBS and ESO binary mixtures was first studied using DSC (Fig. S1). Since no evidence of reaction was noticed, preliminary experiments were conducted to evaluate the thermal reactivity of pure ESO in presence of three different catalysts, Ti(OPr)4), NMI, and MTOAC, each added at 2 % w/w. The resulting binary mixtures were then subject to DSC characterization.

Subsequently, to investigate the reactivity between carboxylic acids and ESO, ternary mixtures were prepared using DA as a model compound (DA/ESO 3:1 molar ratio), in the presence of catalysts (2 % w/w with respect to ESO).

2.3 Extrusion of ternary mixtures: preparation of PBS_ESO blends and films

Once the reaction conditions were optimized, binary (PBS and ESO) and ternary mixtures including PBS, ESO and N-methylimidazole (NMI) as catalyst were extruded. To this aim, PBS pellets were first powdered using a centrifugal mill in liquid N_2 to avoid hydrolytic degradation phenomena, and the resulting powder was kept in an oven at 60 °C under vacuum for 24 h to remove moisture. Then, to ensure good homogeneity of the compounds prior to extrusion, physical mixtures of PBS and ESO (1, 2.5, 5 % w/w) were prepared, with or without NMI (5 % w/w with respect to ESO). For this purpose, ESO (containing 5 % w/w NMI in the case of the catalyzed blends) was first dissolved in

methanol at room temperature under manual stirring, then a suitable amount of the solution was added to PBS powder. The suspensions were mixed, then cast in glass Petri dishes which were put in an oven at 40 °C under vacuum for 24 h to strip off methanol. This preliminary step ensured better dispersion of the components and helped to achieve more uniform blending even using a single extruder pass, thereby minimizing the risk of thermal degradation.

The mixtures were finally thermally processed using a counter-rotating twin screw extruder (HAAKE MiniLab, Thermo Electron Corporation). On the basis of the preliminary DSC and rheological experiments aimed to evaluate the reactivity of DA and ESO in presence of NMI (Section 2.2), the extrusion process was performed at 180 °C and 20 rpm screw speed, which corresponded to a residence time of 1.5–2 min. Depending on the ESO amount and presence of catalysts, six extruded blend samples were obtained, coded as PBS_ESO1, PBS_ESO2.5, PBS_ESO5, PBS_ESO1_NMI, PBS_ESO2.5_NMI, and PBS_ESO5_NMI.

The recovered strands were pelletized, and films were prepared by means of compression molding, using a Carver Laboratory Model C hydraulic press, with the following thermal protocol. The extruded blend was pre-melted at 135 °C at a pressure of 222.2 kPa for 3 min; then pressure was increased to 888.8 kPa for 2 min. Finally, rapid cooling to 50 °C was applied, and after 10 min films with thickness of about 0.2 mm were recovered.

2.4 Characterizations

2.4.1 Rheological properties

The rheological properties of PBS/ESO (1, 2.5, 5 % w/w) physical mixtures were carried out on a stress-controlled Thermo Scientific HAAKE RheoStress 6000 rheometer, equipped with 20 mm diameter parallel plates (gap = 5 mm). The rheological tests were performed in the temperature sweep mode from 130 to 220 °C, with a heating rate of 2 °C/min. The angular frequency and deformation were fixed a 1 rad/s and 10 %.

2.4.2 Fourier transform infrared spectroscopy (FTIR)

Fourier transform infrared spectroscopy (FTIR) in transmission mode was performed using a Perkin Elmer Spectrum 100 spectrometer (Waltham, MA). To avoid signal intensity saturation, FTIR characterization was performed on films about 15 μm thick, obtained by dissolving the extruded PBS_ESO blends in chloroform and evaporating the solvent. Before testing, the samples were dried in an oven at 60 °C for 24 h. The spectroscopic analyses were then performed at room temperature. Spectra were collected as an average of 16 scans in the range of 400–4000 cm^{-1}, with a resolution of 4 cm^{-1}.

2.4.3 Differential scanning calorimetry (DSC)

PBS_ESO and PBS_ESO_NMI extruded blends were investigated using a Q2000 Tzero differential scanning calorimeter (DSC), TA Instrument (New Castle, DE, USA), equipped with a liquid nitrogen accessory for fast cooling. Before DSC analysis, all the samples were dried in an oven under a vacuum at room temperature for 24 h. The calorimeter was calibrated in temperature and energy using indium. Dry nitrogen was used as purge gas at 30 mL/min. DSC measurements were performed on samples of about 5.0 ± 1.0 mg. DSC measurements were performed including double heating runs; the first one, from 25 to 200 °C at 10 °C/min, was followed, after an isothermal step of one minute, by a non-isothermal cooling segment up to –80 °C at a rate of 10 °C/min. Finally, after an isothermal step of one minute, a second heating ramp up to 200 °C at 10 °C/min was recorded. Glass transition temperature (T_g), melt crystallization temperature (T_c), enthalpy of melt crystallization (ΔH_{mc}), melting temperature (T_m), and enthalpy of melting (ΔH_m) were evaluated from the DSC curves.

2.4.4 Thermogravimetry (TG)

A Mettler Toledo TGA/SDTA851e thermo-balance (METTLER-TOLEDO Columbus, Ohio, USA) was used to analyze the thermal stability of the PBS_ESO and PBS_ESO_NMI extruded blends. 6–8 mg of sample were placed in alumina crucibles and heated from 25 to 600 °C at a 20 °C/min rate. The tests were performed in an inert atmosphere with a 30 mL/min nitrogen flow rate. Before testing, the samples were dried under a vacuum for 24 h at room temperature.

2.4.5 Scanning electron microscopy (SEM)

The morphological features of the blend samples were assessed by means of scanning electron microscopy (SEM) (Quanta 200 FEG, 338 FEI, Eindhoven, Netherlands), performed on cryogenically fractured sample cross-sections. SEM micrographs were acquired at room temperature, in high vacuum mode and internal water vapor pressure of 66.7 Pa by using a large-field detector (LFD) and an acceleration voltage of 20 kV. Before the observations, the sample surfaces were coated with a homogeneous layer (18 ± 0.2 nm) of Au and Pd alloy by means of a sputtering device (MED 020, Bal-Tec AG, Tucson, AZ, USA).

2.4.6 Mechanical properties

Tensile tests of the compression molded film samples were carried out following the ISO 37:2017 test method. The measurements were performed using an Instron mod. 4505 dynamometer (Instron Norwood, Massachusetts, USA) equipped with a load cell of 1 kN. The analyses were run at room temperature and 2 mm/min crosshead speed. Dumbbell-shaped specimens (28 mm long, 4 mm wide, and ~0.20 mm thick) were tested. The sample thickness was measured using a digital micrometer (IP65 Mitutoyo, Kawasaki, Japan), and the data were reported as the averaged value of five different measurements. Before performing the tensile tests, the samples were conditioned for 48 h at 25 °C and 50 % RH.

3 Results and discussion

3.1 Reactivity of PBS and ESO: catalyst screening

The reactivity of PBS and epoxidized soybean oil (ESO) was first assessed by DSC and rheological analysis on the powdered PBS/ESO physical mixtures. Fig. S1 reports the non-isothermal DSC thermograms of PBS containing 1, 2.5, 5 % w/w ESO, which clearly highlighted melting and crystallization phenomena of PBS. However, it was not possible to observe any experimental evidence of the chemical reaction between terminal carboxylic groups of PBS and the epoxy group of ESO.

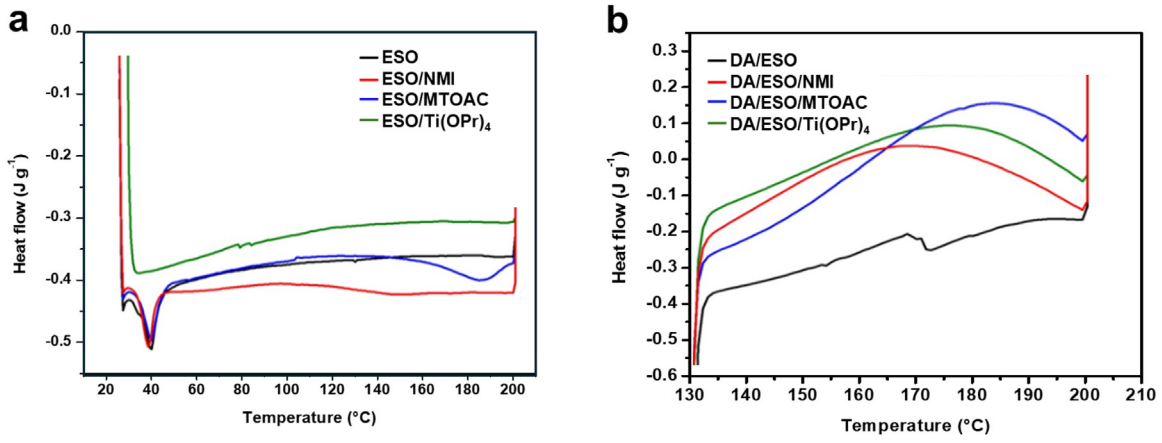

Fig. 1

DSC thermograms of a) ESO containing 2 % w/w of $Ti(OPr)_4$, NMI, and MTOAC, b) DA/ESO 3:1 mol mixtures containing $Ti(OPr)_4$, NMI, and MTOAC (2 % w/w with respect to ESO). Exothermic transitions are in the upward direction.

Therefore, a screening of several catalysts was carried out to choose the most suitable to promote the reaction between PBS and ESO. In particular, three catalysts were tested: $Ti(OPr)_4$, NMI, and MTOAC. $Ti(OPr)_4$ was used because of its efficiency in promoting transesterification reactions [26], NMI was employed for its high reactivity with the epoxy rings in the hardening of epoxy resins [27], while MTOAC is usually used in phase transfers and epoxidation reactions of alkenes, aldehydes, and other classes of compounds [28].

First, the catalyst was mixed with ESO at 2 % w/w, to verify the occurrence of epoxide homopolymerization. The DSC thermograms (Fig. 1a) did not highlight significant thermal events for ESO and ESO/$Ti(OPr)_4$, while very broad and weak exothermic transitions were noted for ESO /NMI and ESO/MTOAC, suggesting the possible occurrence of self-polymerization, even to a very low extent, in the latter cases. Subsequently, in order to assess the most performing catalyst able to promote and hasten PBS and ESO chemical reaction, a model compound, dodecanedioic acid (DA), which bear two terminal carboxyl groups like the employed PBS, was used to simulate the reaction occurring between PBS and ESO. To this aim, DA/ESO 3:1 mol mixtures containing $Ti(OPr)_4$, NMI, and MTOAC (2 % w/w with respect to ESO), were analyzed by DSC (Fig. 1b).

Exothermic peaks in the first heating ramp confirmed the reaction between the carboxylic acid groups and the oxirane rings. Among the tested catalysts, NMI was the most efficient, as evidenced by both the shift of the maximum exothermic peak at lower temperature values and the highest reaction enthalpy (Table 1). For his reason, NMI (5 % w/w with respect to ESO) was chosen as the catalyst to prepare the PBS_ESO reactive blends. To assess the optimal experimental conditions, including temperature and reaction times, to be used during the reactive processing of the PBS/ESO mixtures, the latter were subjected to rheological characterization, both in the presence and absence of NMI.

Temperature sweep tests were performed from 130 to 220 °C with a heating rate of 2 °C/min. The tests provided information regarding the variations in elastic and loss moduli (G' and G'') and complex viscosity (η^*) of the systems under examination. Fig. 2a illustrates the curves related to the PBS/ESO mixtures devoid of any catalyst. All samples exhibited a decreasing trend in G', G'', and η^* (Fig. S2a) with increasing temperature due to the weakening of the intermolecular forces upon heating. It was also noticed that the viscoelastic properties decreased with the increase in the percentage of ESO, supporting the hypothesis of a mild plasticizing effect of ESO on PBS. However, at temperatures close to 200 °C a slight increase in G' was observed for the mixtures with the higher contents of ESO, possibly related to the inception of intermolecular chain extension processes of PBS. The difference between the viscoelastic properties of pristine PBS and those of the mixtures with ESO became dramatically more pronounced in samples containing NMI. As shown in Fig. 2b, at around 180 °C all samples except PBS exhibited a clear discontinuity in the decreasing trend of G', which started to increases significantly with temperature. This trend became more pronounced with higher contents of ESO. In particular, in the 5 % mixture, a remarkable increase in G'' (1 order of magnitude over PBS at 220 °C) and complex viscosity was also observed (Fig. S2b) which corroborated the occurrence of the chain extension reaction between PBS and ESO [29]. A further confirmation of the occurrence of the PBS chain extension was provided by the second scan of the PBS/ESO5/NMI mixture, which exhibited significantly enhanced viscoelastic properties. Indeed, its G' values were higher than those of PBS over the entire investigated range of temperature, with a difference of about 2 orders of magnitude at 200 °C (Fig. 2b). Furthermore, a

Table 1

Thermal parameters of the reaction between DA and ESO in presence of different catalysts.

Catalyst	T_{max} (°C)	ΔH (J/g)
$Ti(OPr)_4$	173.6	49.1
NMI	166.7	55.7
MTOAC	183.2	54.2

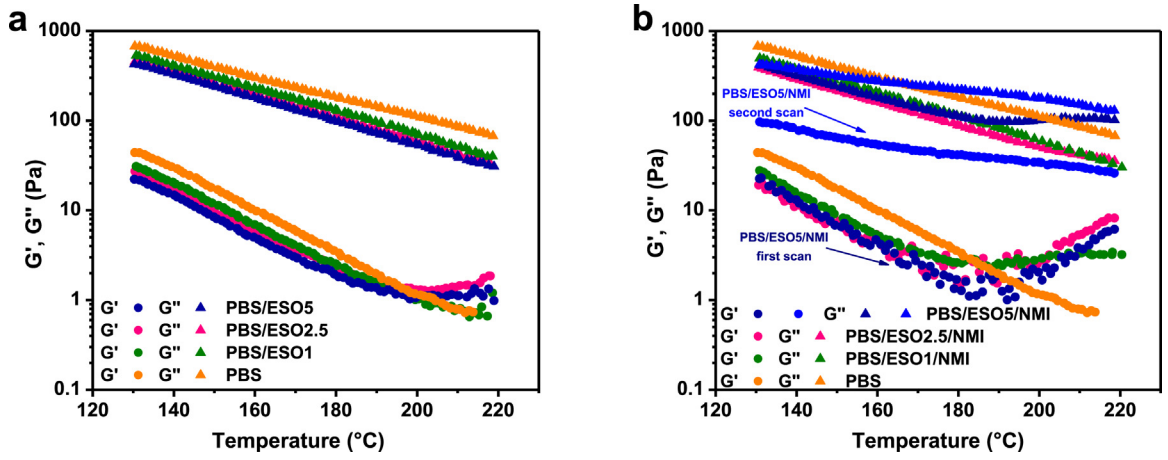

Fig. 2

Rheological characterization of the PBS/ESO mixtures. Temperature sweep tests of a) PBS/ESO physical mixtures and b) PBS/ESO physical mixtures containing NMI. The light blue traces refer to the second heating scan of PBS/ESO5/NMI.

shift in the phase angle, from 88 (PBS/ESO5/NMI, first scan) to 78° (PBS/ESO5/NMI, second scan), indicated an increased elastic behavior of the melt-reacted blend [30]. Overall, this evidence confirmed the occurrence of the chain extension reaction which led to the formation of a PBS-*co*-ESO copolymer, resulting in increased viscoelastic properties and phase compatibility of the PBS_ESO reactive blends (see also Section 3.5).

Since the rheological analysis revealed that the reaction took place at around 180 °C, this temperature value was chosen in the subsequent extrusion process. To this aim, the powder mixtures were processed with a counter-rotating extruder on a lab scale, and the extruded samples were characterized by FT-IR spectroscopy, DSC, TGA, and morphological analyses (SEM), while compression molded films were subject to mechanical testing. The results obtained are reported in the following sections.

3.2 Fourier transform infrared spectroscopy (FTIR) of PBS_ESO blends

FTIR spectroscopy was used to probe the possible reaction occurring between PBS and ESO during the reactive blending process, both with and without NMI as a catalyst. The FTIR spectra of neat PBS and ESO are reported in Fig. 3, along with the spectra of the samples containing 5wt% ESO. In the wavenumbers range of 3600–2800 cm^{-1} the stretching of -OH bonding (3400–3000 cm^{-1}) and the characteristic -CH group stretching signals (3000–2800 cm^{-1}) were noticed (Fig. 3a, b) [17,31]. A weak absorption at 3450 cm^{-1} in ESO spectrum might be due to water absorption, while two high-intensity peaks at 2926 and 2856 cm^{-1} correspond to the hydrocarbon chain stretching of the backbone [5,9]. Furthermore, the absorption of the carbonyl ester group (C=O) was observed at 1745 cm^{-1} (Fig. 3b). In the PBS spectrum, additional hydrocarbon stretching absorptions were noted at 2968 and 2950 cm^{-1} due to C–H asymmetric vibration of free and rigid amorphous phase. Carbonyl absorptions could be evidenced by the peaks at 1740, 1720 and 1711 cm^{-1}, corresponding to the free amorphous phase and less ordered and hydrogen bonded crystalline polymer fractions, respectively [32]. Finally, in the fingerprint region of ESO, the peaks found at 1240, 825, 843, and 780 cm^{-1}, related to C–O–C oxiranic group stretching, and the bands at 723 and 1470 cm^{-1}, associated with C–C stretching, indicated the presence of the epoxy ring (Fig. 3a) [33].

In the PBS_ESO systems, an absorbance increase of the –OH stretching (3400–3100 cm^{-1}) was noticed, which was further enhanced in the presence of NMI, indicating the formation of hydroxyl groups due to the epoxy ring opening [34] (Fig. 3b). The carbonyl region was poorly affected, even though a broadening of the band was observed at higher wavenumbers (Fig. 3c) due to the presence of the ESO ester linkages. The addition of ESO in PBS_ESO5 caused the broadening to higher wavenumbers of the band of PBS at 820 cm^{-1} and the appearance of a slight absorption at 830 cm^{-1}. This evidence was related to C–O–C oxiranic ring vibrational motions, which shifted to lower values with respect to ESO (843 and 825 cm^{-1}) (Fig. 3d). The shift of the bands towards lower values could be due to physical interaction between polar groups of PBS and oxirane oxygen through the formation of hydrogen bonds inhibiting the vibrational motions associated to the stretching of ESO C–O–C group. Notably, the band at 830 cm^{-1} disappeared in PBS_ESO5_NMI, further confirming that the addition of NMI promoted the epoxy ring opening reaction, triggering the chain extension reaction between ESO and PBS.

3.3 Differential scanning calorimetry of PBS_ESO blends

The DSC curves related to cooling run and second heating and of PBS_ESO and PBS_ESO_NMI blend samples are reported in Fig. 4, while DSC parameters are listed in Table 2. All curves related to the uncatalyzed systems (Fig. 4a) showed crystallization phenomenon due to homogeneous packing of macromolecules, with a comparable temperature onset. A shift of the crystallization peak temperature (T_c) and the outset toward lower values was observed for the samples containing ESO. In this case ESO acted as a plasticizer, allowing the chain rearrangement of the polymer chains even at temperatures lower than 80 °C, where the mobility of neat PBS is restricted. This effect was able to modulate the crystallization process, causing it to occur over

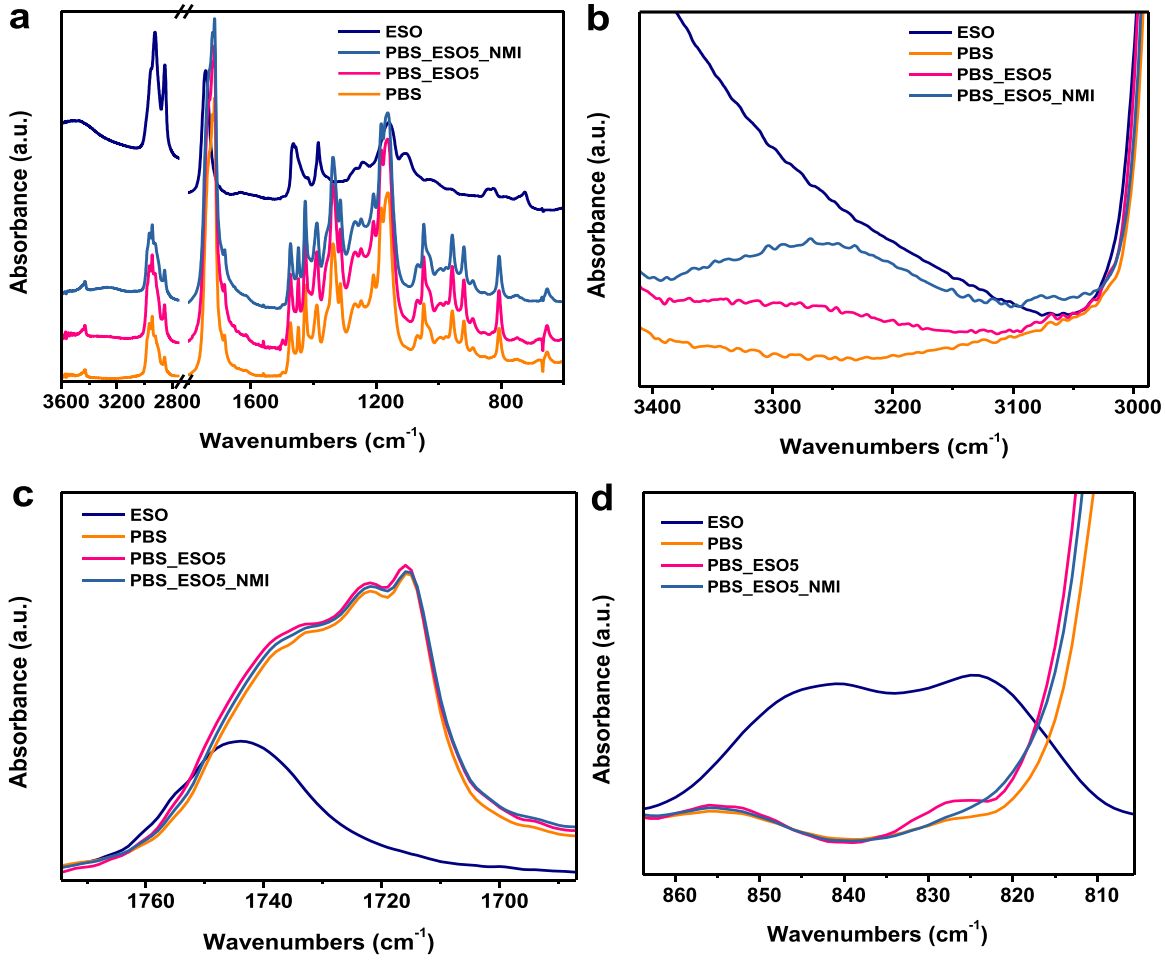

Fig. 3

FTIR spectra of ESO, PBS, PBS_ESO5 and PBS_ESO5_NMI blends. a) full wavenumbers range, and closeup of b) hydroxyl stretching region, c) carbonyl region, d) epoxy absorption region.

Table 2

Thermal parameters of neat PBS, PBS_ESO, and PBS_ESO_NMI systems.

Sample	Thermogravimetry		Differential scanning calorimetry				
	$T_{onset,10\ \%WL}$* (°C)	T_{peak}# (°C)	T_g (°C)	T_c (°C)	ΔH_c (J/g)	T_m (°C)	$\Delta H_{m,tot}$ (J/g)
PBS	340.6	393.6	−34.2	84.6	59.8	113.7	−48.0
PBS_ESO1	345.4	400.3	−33.1	83.0	64.3	113.1	−51.7
PBS_ESO2.5	344.0	403.0	−32.2	83.2	66.2	113.1	−53.6
PBS_ESO5	338.6	388.3	−34.8	83.5	64.3	113.2	−52.6
PBS_ESO1_NMI	342.0	401.6	−32.5	82.7	65.7	113.1	−55.1
PBS_ESO2.5_NMI	342.7	399.0	−33.9	82.9	65.8	113.2	−54.9
PBS_ESO5_NMI	348.5	404.6	−34.1	82.8	64.4	113.7	−53.2

* WL – weight loss;
\# from derivative thermogravimetry.

a larger temperature range. The impact of ESO could be also seen by the increasing ΔH_c values of all PBS_ESO samples compared to the neat PBS. These evidences suggest that ESO does not substantially influence the structural reorganization of the polymer chains during cooling, but is able to promote completion of crystallization due to the favored chain rearrangement during the process [35]. The promotion of the development of crystalline phase can result in improved mechanical properties of PBS [36]. This outcome was indeed confirmed by tensile tests results discussed in Section 3.4.

From the analysis of the DSC thermograms during the second heating ramp (Fig. 4b), it was also possible to observe two melting

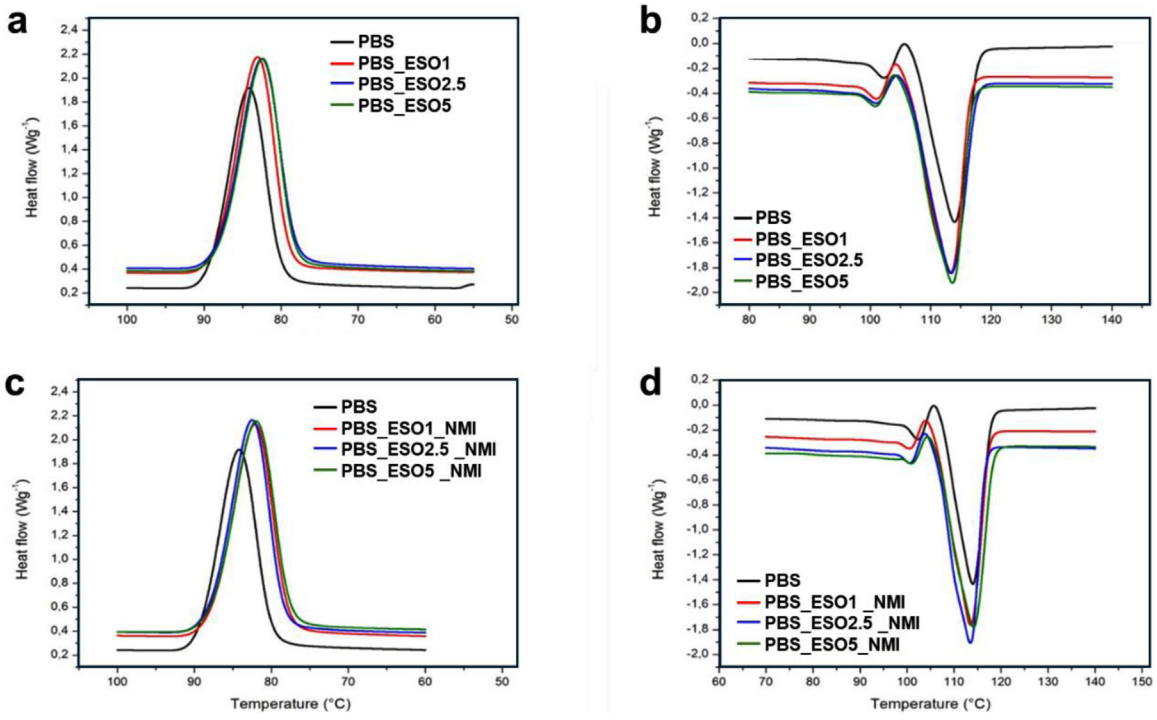

Fig. 4

DSC thermograms of PBS_ESO blends. Cooling steps of a) PBS_ESO, and c) PBS-ESO_NMI blends. Second heating step of b) PBS_ESO, and d) PBS_ESO_NMI blends.

peaks and one crystallization peak. Several studies report that different crystallization rates by the melted polymeric chains are responsible for the presence of multiple fusion endotherms in the second heating ramp [31,37-38]. For the neat PBS sample it is noted that the crystallization exotherm during heating is associated with the *"melting-recrystallization-remelting"* model. In this case, some crystalline lamellae of different thicknesses and sizes, formed during the melt cooling process, are characterized by low thermal stability. For this reason, the crystalline lamellae melt in the second heating ramp and reorganize into metastable crystalline forms, becoming more susceptible to the subsequent melting process [37,39]. Due to this complex phenomenon, the melting enthalpy values were lower than the corresponding ΔH_c values.

Regarding the PBS_ESO systems, it was noted that the onset temperature of the melting peak of the binary blends decreased by about 4 °C compared to neat PBS, due to the higher mobility of the PBS chains in the presence of ESO (Fig. 4b). However, smaller differences in the maximum of the melting peak temperature were noted, since the polymer structure was not substantially influenced (Table 2).

The ternary PBS_ESO_NMI blends showed a trend similar to the PBS_ESO systems during cooling and heating (Fig. 4c and d). However, in PBS_ESO_NMI samples, the crystallization peak further shifted to lower temperatures, suggesting that the occurrence of the chemical reaction between PBS and ESO upon extrusion could further affect the crystallization behavior of PBS. On the other hand, the glass transition temperature (T_g) values of PBS were comparable to those of PBS_ESO_NMI and PBS_ESO.

3.4 Thermogravimetry (TG) of PBS_ESO blends

Thermogravimetry provided information on the PBS-based blends thermal stability as a function of temperature under inert atmosphere. Fig. 5 displays TG curves of the PBS_ESO extruded blends. The characteristic thermal parameters measured included onset temperature (T_{onset}), taken as the temperature at which 10 % weight loss (W_L) of sample occurred, and maximum degradation temperature (T_{max}), which was calculated as the temperature at the maximum of the derivative thermogravimetric (DTG) curve (Table 2). Interestingly, PBS_ESO1 and PBS_ESO2.5 (Fig. 5a) displayed higher onset degradation temperatures ($T_{onset,10\ \%WL}$) and maximum degradation peaks (T_{peak}) with respect to neat PBS (Table 2), indicating an increase in thermal stability.

This outcome was rather unexpected, since plasticizers usually induce an increase of macromolecular mobility, promoting in this way the degradation of the polymer [40]. In the present case, rheological characterization demonstrated that PBS and ESO can react above 200 °C even in the absence of catalyst, leading to the formation of a chain-extended copolymer endowed with higher thermal stability. A similar feature has been also observed for PLA containing acrylated ESO [41]. An opposite effect was evidenced in PBS_ESO5, where both $T_{onset,10\ \%WL}$ and T_{peak} decreased. In this case, it could be hypothesized that the excess of additive could both foster the plasticization effect, thus promoting PBS thermal degradation, as well as induce phase segregation of the unreacted ESO in larger microdomains (see Section 3.5), encouraging its evaporation and the thermal transfer from the outside.

All PBS_ESO_NMI blends displayed higher $T_{onset,10\ \%WL}$ and T_{peak} with respect to neat PBS (Fig. 5b and Table 2), confirming the positive effect of ESO on the thermal stability of PBS. No

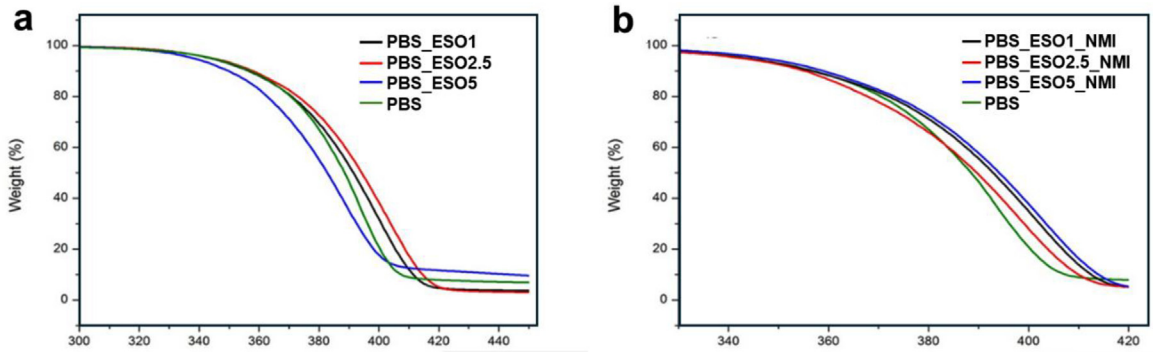

Fig. 5

Thermogravimetric curves (TG) of a) PBS_ESO, and b) PBS_ESO_NMI blend systems.

significant differences were observed comparing the data relative to uncatalyzed and catalyzed blends containing 1 or 2.5 w/w ESO, suggesting that low amounts of ESO could completely react with PBS even in the absence of catalyst. However, for increased ESO contents, the presence of NMI was necessary in order to enhance thermal stability. Indeed, PBS_ESO5_NMI exhibited the highest $T_{onset,10\,\%WL}$ and T_{peak} values, which were 10 and 6 °C higher, respectively, than those of the uncatalyzed PBS_ESO5 sample (Table 2). This evidence indicates that for ESO amounts as high as 5 % w/w, NMI was needed to complete the chain extension reaction between polymer and oil, which resulted in increased compatibility of the otherwise poorly miscible PBS and ESO phases, and enhanced thermal stability of the polymer formulation.

Table 3

Mechanical properties of PBS, PBS_ESO, and PBS_ESO_NMI films.

Film samples	Young's modulus (MPa)	Tensile strength (MPa)	Elongation at break (%)
PBS	666 ± 43	22.5 ± 2.2	7.3 ± 0.3
PBS_ESO1	682 ± 38	23.3 ± 1.8	7.3 ± 0.2
PBS_ESO2.5	597 ± 35	19.1 ± 1.1	7.9 ± 0.2
PBS_ESO5	621 ± 36	20.8 ± 1.3	9.0 ± 0.1
PBS_NMI	643 ± 71	22.8 ± 3.9	7.4 ± 0.4
PBS_ESO1_NMI	775 ± 34	24.3 ± 2.0	7.1 ± 0.2
PBS_ESO2.5_NMI	633 ± 29	23.9 ± 0.9	7.5 ± 0.3
PBS_ESO5_NMI	663 ± 11	24.0 ± 1.1	8.0 ± 0.2

3.5 Scanning electron microscopy (SEM) of PBS_ESO blends

The morphological analysis of the fractured cross sections of the blends (Fig. 6) highlighted the presence of spherical voids observed in the micrographs of PBS_ESO, which resulted from the formation of oil droplets within the polymer matrix during blending, and their removal occurring during the cryogenic sample surface fracture (Fig. 6 a,c,e) and SEM observation. In addition, the size and number of epoxidized soybean oil domains steadily increased with the oil concentration. This outcome evidenced the poor compatibility between PBS and ESO, although the relatively homogeneous distribution of the microdomains inside the polymeric matrix suggested the existence of interfacial interactions between the two phases [42].

The morphological analysis of the cross section of PBS_ESO_NMI samples revealed a significantly different appearance (Fig. 6 b,d,f). The sample surface was more homogeneous and a drastic reduction of both interstitial cavity concentration and micro-domains was evident. The morphological analysis of the PBS_ESO_NMI system underlined a better interfacial adhesion and compatibility between the polymer and the oil with respect to the PBS_ESO systems. This outcome confirmed the occurrence of the reaction between PBS and ESO, which resulted in a remarkable increase in the compatibilization of the two phases. This outcome well matched with the data obtained from rheological characterization and TG previously discussed.

3.6 Mechanical properties of PBS_ESO blend films: tensile tests

The tensile stress-strain curves of pure PBS, PBS containing 0.25 % w/w NMI (PBS_NMI), PBS_ESO, and PBS_ESO_NMI compression molded films with different ESO loadings are represented in Fig. S3, while the tensile properties calculated are listed in Table 3. In comparison to neat PBS, the tensile strength and Young's modulus for the PBS_ESO blends decreased with increasing ESO contents, except for the PBS_ESO1, where tensile strength and Young's modulus increased from 666.5 MPa and 22.5 MPa, to 682.5 MPa and 23.3 MPa, respectively. This evidence suggests that increasing concentrations of ESO weakened the interactions among the PBS chains, resulting in a decrease in both PBS tensile strength and Young's modulus [35]. The elongation at break of the PBS_ESO films was higher than that of pure PBS (7.3 %), and the highest value of elongation at break was observed for PBS_ESO5 (9.0 %), indicating that ESO improved the flexibility and ductility of PBS chains, slightly increasing their plasticity. In general, a plasticizer weakens the interaction between polymers chains and causes an improvement in the flexibility of polymer, which results in lower modulus and increased elongation at break values [36]. However, to elicit a relevant effect, typical plasticizer levels in PBS blends should be above 10 % w/w [43], while lower amounts can induce antiplasticization, which even increases stiffness [44]. In the case of the binary PBS_ESO1 blend, higher tensile strength and Young's modulus values were due to the antiplasticization effect. Increasing concentrations of ESO did actually favored

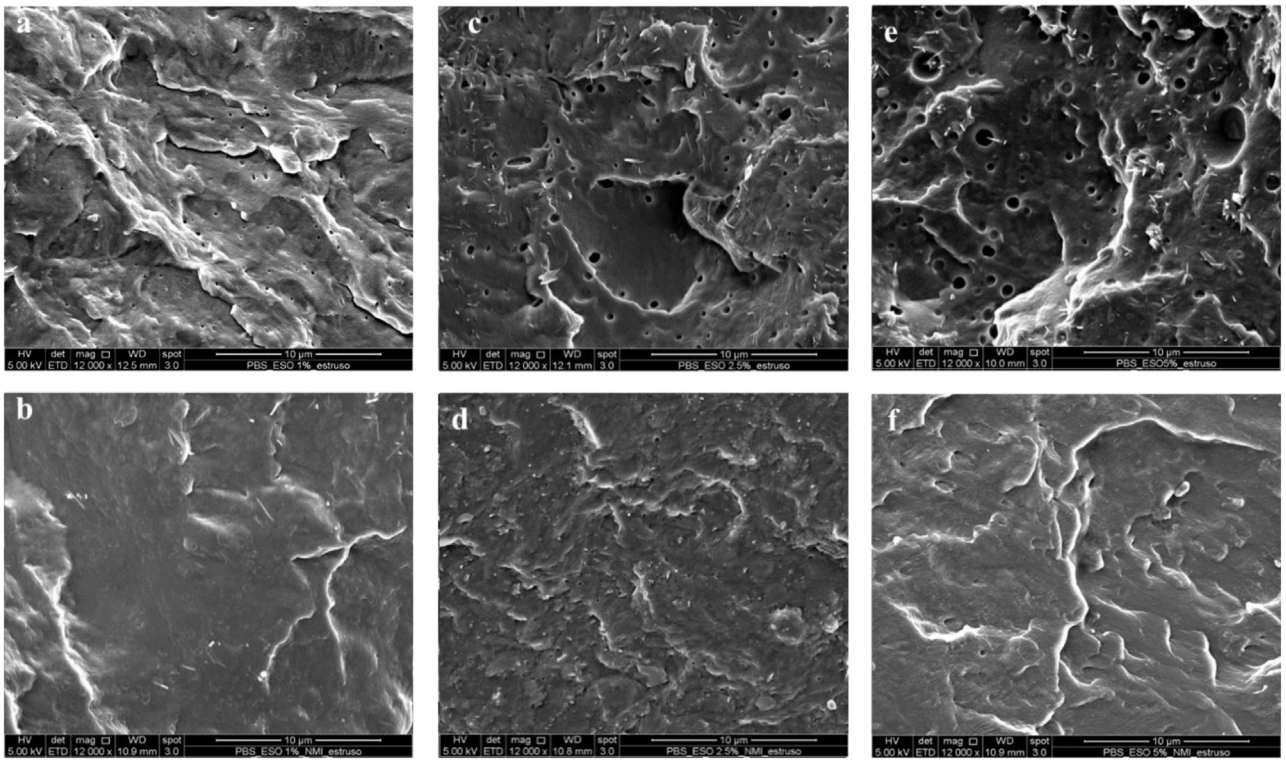

Fig. 6

SEM images of the cross sections of PBS_ESO blend. a) PBS_ESO1, c) PBS_ESO2.5, e) PBS_ESO5, b) PBS_ESO1_NMI, d) PBS_ESO2.5_NMI, f) PBS_ESO5_NMI.

plasticization of the blends, however the effect was moderate, as ESO contents exceeding 5 % caused oil blooming to the film surface due to the poor phase compatibility.

The addition of 0.25 % w/w of NMI in PBS did not impart significant differences in mechanical properties, ruling out the occurrence of PBS condensation reactions. As concerning the PBS_ESO_NMI film systems, they resulted stiffer than the counterparts without catalysts, as increased tensile strength and moduli were noted compared to neat PBS and PBS_ESO samples. In particular, PBS_ESO1_NMI presented the highest tensile strength and modulus values. In general, during the chain extension reaction between PBS and ESO, NMI induced the formation of new polymer linkages, with possible branching, increasing the capacity of materials to bear the tensile stress before breaking. Notably, the film ductility was not impaired. These properties are promising with a view of using these systems in the semi-flexible packaging sector to realize biodegradable plastic containers.

4 Conclusions

In the scope of this work, systems based on PBS and ESO at different concentrations, both in the presence and absence of NMI, were studied. NMI was selected as a catalyst after a preliminary DSC study of the reaction between ESO and dodecanedioic acid. All the findings, in terms of rheological tests, spectroscopic analysis, morphological and thermal properties, and mechanical performances, provided interesting insights on the mutual reactivity of PBS and ESO in presence of NMI, suggesting the formation of a tight and complex network, in which ESO was well embedded in PBS polymer matrix. The addition of ESO enabled to modulate chain mobility, crystallization, and the melting point of the polymer matrix, also resulting in an increase in polymer thermal stability and mechanical stiffness. Furthermore, a mild plasticizing effect, commensurate with the low amount of ESO in the blends, was observed. These insights highlight the promising perspective for the creation of innovative biodegradable materials with tunable properties, which could be addressed to application meeting both the ever changeable needs of industries and the environmental concerns, such as the development of sustainable materials for biodegradable packaging. To this aim, further research should be focused on the improvement and optimization of formulations and processing parameters of these systems to fine-tune their properties for specific applications. First, a deeper quantitative analysis of the achieved chain extension should be assessed by analysing the molecular weight increase by GPC characterization of the blends. Additionally, exploring potential scalability and assessing the long-term stability and biodegradability of these materials would be essential steps in realizing their full potential in handling sustainability challenges in packaging and beyond.

Declaration of competing interest

The authors declare that they have no known competing financial interests or personal relationships that could have appeared to influence the work reported in this paper.

Data Availability

Data will be made available on request.

CRediT authorship contribution statement

Rosa Turco: Conceptualization, Supervision, Writing – review & editing. **Salvatore Mallardo:** Investigation, Data curation. **Domenico Zannini:** Investigation, Data curation, Writing – original draft. **Arash Moeini:** Validation, Writing – review & editing. **Martino Di Serio:** Supervision, Funding acquisition. **Riccardo Tesser:** Supervision. **Pierfrancesco Cerruti:** Conceptualization, Writing – review & editing, Funding acquisition. **Gabriella Santagata:** Conceptualization, Writing – review & editing, Supervision.

Acknowledgments

The authors thank the Extended Partnership PE00000004 "Made in Italy Circolare e Sostenibile" (MICS) project, funded by the European Union-Next Generation EU, and project SisTEmi multifunzionali nanofibrosi per controllare e riduRRE gli impatti ambientali nei sistemi agricoli (TERRE) Progetti@CNR SAC.AD002.173.41 for their financial support. The European Union's Horizon 2020 research and innovation program (PRIMA call) partially funded the current work under grant agreement no. 02WPM1683, EU Project, "From Edible Sprouts to hEalthy food -FEED".

The authors also express their gratitude to Dr. Federica Ronca for her keen dedication during her bachelor thesis on the research topic.

Supplementary materials

Supplementary material associated with this article can be found, in the online version, at doi:10.1016/j.giant.2024.100328.

References

[1] M. Rolf, Green polymer chemistry and bio-based plastics: dreams and reality, Macromolecul. Chem. Phys. 214 (2013) 159–174.

[2] M. Dobrzyńska-Mizera, M. Knitter, M. Piss, C. Del Barone, S. Mallardo, G. Santagata, M.L. Di Lorenzo, Thermal and Morphological Analysis of Linear Low-Density Polyethylene Composites Containing d-limonene/β-cyclodextrin for Active Food Packaging, Molecules 28 (3) (2023) 1120.

[3] P.N.T. Pilapitiya, A.S. Ratnayake, The world of plastic waste: a review, Clean. Mater. (2024) 100220.

[4] J. Xu, B.-H. Guo, Poly(butylene succinate) and its copolymers: Research, development and industrialization, Biotechnol. J. 5 (2010) 1149–1163.

[5] A.R. de Matos Costa, A. Crocitti, L.H. de Carvalho, S.C. Carroccio, P. Cerruti, G. Santagata, Properties of biodegradable films based on poly(butylene succinate) (PBS) and poly(butylene Adipate-co-Terephthalate) (PBAT) blends, Polymers 12 (10) (2020).

[6] A. Moeini, N. Germann, M. Malinconico, G. Santagata, Formulation of secondary compounds as additives of biopolymer-based food packaging: a review, Trend. Food Sci. Technol. 114 (2021) 342–354.

[7] M. Dobrzyńska-Mizera, M. Knitter, S. Mallardo, M.C. Del Barone, G. Santagata, M.L. Di Lorenzo, Thermal and thermo-mechanical properties of poly(L-lactic acid) biocomposites containing β-cyclodextrin/d-limonene inclusion complex, Materials 14 (10) (2021).

[8] M. Dobrzyńska-Mizera, M. Knitter, D. Szymanowska, S. Mallardo, G. Santagata, M.L. Di Lorenzo, Optical, mechanical, and antimicrobial properties of bio-based composites of poly(L-lactic acid) and D-limonene/β-cyclodextrin inclusion complex, J. Appl. Polym. Sci. 139 (20) (2022).

[9] S. Mallardo, V. De Vito, M. Malinconico, M.G. Volpe, G. Santagata, M.L. Di Lorenzo, Poly(butylene succinate)-based composites containing β-cyclodextrin/d-limonene inclusion complex, Eur. Polym. J. 79 (2016) 82–96.

[10] A.K. Mohanty, M. Misra, L.T. Drzal, Sustainable bio-composites from renewable resources: opportunities and challenges in the green materials world, J. Polym. Environ. 10 (2002) 19–26 N. B. Samarth and A. Mahanwar, Modified Vegetable Oil Based Additives as a Future Polymeric Material-Review, Open Journal of Organic Polymer Materials, 5, 1, 2015.

[11] N. Jacquel, F. Freyermouth, F. Fenouillot, A. Rousseau, J.P. Pascault, P. Fuertes, R. Saint-Loup, Synthesis and properties of poly(butylene succinate): Efficiency of different transesterification catalysts, J. Polym. Sci. Part A: Polym. Chem. 49 (2011) 5301–5312.

[12] N. Lin, D. Fan, R. Chang, J. Yu, X. Cheng, J. Huang, Structure and properties of poly(butylene succinate) filled with lignin: a case of lignosulfonate, J. Appl. Polym. Sci. 121 (2011) 1717–1724.

[13] C.I. Gkountela, D. Markoulakis, M. Mathioudaki, I. Pitterou, A. Detsi, S:N. Vouyiouka, Scalable enzymatic polymerization and low-temperature post-polymerization of poly (butylene succinate): process parameters and application, Eur. Polym. J. 198 (2023) 112423.

[14] M. Barletta, C. Aversa, M. Ayyoob, A. Gisario, K. Hamad, M. Mehrpouya, H. Vahabi, Poly (butylene succinate)(PBS): materials, processing, and industrial applications, Progr. Polym. Sci. 132 (2022) 101579.

[15] V. Marturano, A. Marotta, S. Agustin Salazar, V. Ambrogi, P. Cerruti, Recent advances in bio-based functional additives for polymers, Progr. Mater. Sci. 139 (2023).

[16] S. Chuakhao, J.T. Rodríguez, S. Lapnonkawow, G. Kannan, A.J. Müller, S. Suttiruengwong, Formulating PBS/PLA/PBAT blends for biodegradable, compostable packaging: the crucial roles of PBS content and reactive extrusion, Polym. Test. 108383 (2024).

[17] A.K. Mohanty, M. Misra, L.T. Drzal, Sustainable bio-composites from renewable resources: opportunities and challenges in the green materials world, J. Polym. Environ. 10 (2002) 19–26.

[18] J.B. Zhao, K.Y. Li, W.T. Yang, Chain extension of polybutylene adipate and polybutylene succinate with adipoyl-and terephthaloyl-biscaprolactamate, J. Appl. Polym. Sci. 106 (2007) 590–598.

[19] C. Hiemenz, T. Lodge, Polymer Chemistry, Engineering & Technology, Physical Sciences, 2007.

[20] E. Santacesaria, R. Tesser, M. Di Serio, R. Turco, V. Russo, D. Verde, A biphasic model describing soybean oil epoxidation with H_2O_2 in a fed-batch reactor, Chem. Eng. J. 173 (1) (2011) 198–209.

[21] R. Ortega-Toro, G. Santagata, G. Gomez d'Ayala, P. Cerruti, P. Talens Oliag, M.A. Chiralt Boix, M. Malinconico, Enhancement of interfacial adhesion between starch and grafted poly(ε-caprolactone), Carbohyd. Polym. 147 (2016) 16–27.

[22] H. Dai, L. Yang, B. Lin, C. Wang, G. Shi, Synthesis and characterization of the different soy-based polyols by ring opening of epoxidized soybean oil with methanol, 1,2-ethanediol and 1,2-propanediol, J. Am. Oil Chemist. Soc. 86 (2009) 261–267.

[23] Z. Ma, T. Yin, Z. Jiang, Y. Weng, C. Zhang, Bio-based epoxidized soybean oil branched cardanol ethers as compatibilizers of polybutylene succinate (PBS)/polyglycolic acid (PGA) blends, Int. J. Biolog. Macromolecul. 259 (2024) 129319.

[24] A. Alhanish, M. Abu Ghalia, Developments of biobased plasticizers for compostable polymers in the green packaging applications: a review, Biotechnol. Progr. 37 (2021) e3210.

[25] R. Turco, R. Tesser, M.E. Cucciolito, M. Fagnano, L. Ottaiano, S. Mallardo, M. Malinconico, G. Santagata, M. Di Serio, Cynara cardunculus biomass recovery: an eco-sustainable, nonedible resource of vegetable oil for the production of poly(lactic acid) bioplasticizers, ACS Sustain. Chem. Eng. 7 (4) (2019) 4069–4077.

[26] N. Jacquel, F. Freyermouth, F. Fenouillot, A. Rousseau, J.P. Pascault, P. Fuertes, R. Saint-Loup, Synthesis and properties of poly(butylene succinate): Efficiency of different transesterification catalysts, J. Polym. Sci. Part A: Polym. Chem. 49 (2011) 5301–5312.

[27] A. Farkas, P.F. Strohm, Imidazole catalysis in the curing of epoxy resins, J. Appl. Polym. Sci. 12 (1968) 159–168.

[28] C.M. Starks, Phase-transfer catalysis. I. Heterogeneous reactions involving anion transfer by quaternary ammonium and phosphonium salts, J. Am. Chem. Soc. 93 (1971) 195–199.

[29] Q.-y. Ge, Q. Dou, Preparation of supertough polylactide/polybutylene succinate/epoxidized soybean oil bio-blends by chain extension, ACS Sustain. Chem. Eng. 11 (2023) 9620–9629.

[30] A. Avella, R. Mincheva, J.-M. Raquez, G. Lo Re, Substantial effect of water on radical melt crosslinking and rheological properties of poly(ε-caprolactone), Polymers 13 (2021) 491.

[31] I. Vroman, L. Tighzert, Biodegradable polymers, Materials 2 (2009) 307–344.

[32] S.-F. Yao, X.-T. Chen, H.-M. Ye, Investigation of structure and crystallization behavior of poly(butylene succinate) by Fourier transform infrared spectroscopy, J. Phys. Chem. B 121 (2017) 9476–9485.

[33] N. Chen, P. Zheng, Q. Zeng, Q. Lin, J. Rao, Characterization and performance of soy-based adhesives cured with epoxy resin, Polymers 9 (2017) 514.

[34] T. Hansen, Vermeeren, A. Haim, M.J.H. van Dorp, D.J.D.C. Codée, D.F.M. Bickelhaupt, D.T.A. Hamlin, Regioselectivity of epoxide ring-openings via SN2 reactions under basic and acidic conditions, Eur. J. Organ. Chem. (2020) 3822–3828.

[35] F. Ali, Y.-W. Chang, S.C. Kang, J.Y. Yoon, Thermal, mechanical and rheological properties of poly (lactic acid)/epoxidized soybean oil blends, Polym. Bull. 62 (2009) 91–98.

[36] Y. Zhao, J. Qu, Y. Feng, Z. Wu, F. Chen, H. Tang, Mechanical and thermal properties of epoxidized soybean oil plasticized polybutylene succinate blends, Polym. Adv. Technolog. 23 (2012) 632–638.

[37] R. Pfaendner, How will additives shape the future of plastics? Polym. Degradat. Stabil. 91 (2006) 2249–2256.

[38] R. Dragana, N.M.S. Marija, Đ. Jasna, The influence of antioxidant and post-synthetic treatment on the properties of biodegradable poly(butylene succinate)s modified with poly(propylene oxide), J. Serb. Chem. Soc. 72 (2007) 1515–1531.

[39] X. Wang, L. Song, H. Yang, H. Lu, Y. Hu, Synergistic effect of graphene on antidripping and fire resistance of intumescent flame retardant poly(butylene succinate) composites, Ind. Eng. Chem. Res. 50 (2011) 5376–5383.

[40] R. Turco, D. Zannini, S. Mallardo, G. Dal Poggetto, R. Tesser, G. Santagata, M. Malinconico, M. Di Serio, Biocomposites based on Poly(lactic acid), Cynara Cardunculus seed oil and fibrous presscake: a novel eco-friendly approach to hasten PLA biodegradation in common soil, Polym. Degradat. Stabil. 188 (2021).

[41] L. Quiles-Carrillo, S. Duart, N. Montanes, S. Torres-Giner, R. Balart, Enhancement of the mechanical and thermal properties of injection-molded polylactide parts by the addition of acrylated epoxidized soybean oil, Mater. Des. 140 (2018) 54–63.

[42] W. Dong, B. Zou, Y. Yan, Ma, M. Chen, Effect of chain-extenders on the properties and hydrolytic degradation behavior of the poly(lactide)/poly(butylene adipate-co-terephthalate) blends, Int. J. Molecul. Sci. 14 (10) (2013) 20189–20203.

[43] B.Y. Hou, L. Ren, D.M. Fu, Y.Y. Jiang, M.Y. Zhang, H.X. Zhang, Novel environmentally sustainable xylitol-based plasticizer: synthesis and application, J. Polym. Res. 28 (2021) 1–12.

[44] L. Mascia, Y. Kouparitsas, D. Nocita, X. Bao, Antiplasticization of polymer materials: Structural aspects and effects on mechanical and diffusion-controlled properties, Polymers 12 (769) (2020).